Generation of Global Backscatter Maps for Future SAR Missions Design

Luca Dell'Amore[1], José-Luis Bueso-Bello[1], Michele Martone[1], and Paola Rizzoli[1]
[1]Microwaves and Radar Institute, German Aerospace Center (DLR), Wessling, Germany

Abstract

The generation of global backscatter maps allows for the exploitation of a priori knowledge of local synthetic aperture radar (SAR) backscatter statistics. SAR backscatter maps can be used for accurate performance prediction and for the optimization of instrument settings for present and future SAR systems. Also, many further SAR applications can benefit from the availability of backscatter maps in order to monitor the backscatter evolution in time and to investigate the radar reflectivity behaviour depending on sensor parameters and target properties. In this work, X-band backscatter maps are generated by mosaicking images acquired by the TerraSAR-X (TSM) and the TanDEM-X (TDM) missions at global scale. The correction models used for the characterization of backscatter behaviour are based on the database provided by Ulaby in [3] and are here presented for HH polarization and for any required reference incidence angle. As an example of application for future SAR missions design, a novel performance-optimized block-adaptive quantization (PO-BAQ), coming from the need of optimizing the resource allocation of the state-of-the-art quantization algorithms for SAR systems, is then considered. The methodology relies on global backscatter statistics for the generation of bitrate maps, which can provide a helpful information for performance budget definition and for optimizing resource allocation strategies.

1 Introduction

Synthetic aperture radar (SAR) systems represent nowadays a well-recognized technique in the field of remote sensing. They are able to acquire high-resolution images of the Earth's surface, independently of daylight and weather conditions, and provide useful data for a large number of scientific applications, such as hydrology, glaciology, forestry, and oceanography. Precise a priori backscatter knowledge is necessary for an optimized operation of SAR systems in order to automatically adapt radar parameters on-board during a data take. For realistic performance prediction of future SAR systems, the backscatter information represents a valuable input, e.g., for signal-to-noise ratio (SNR) estimation or data clipping values computation. Moreover, many further SAR applications can benefit from the availability of backscatter maps, such as the monitoring of backscatter evolution in time and the investigation of radar reflectivity depending on land type and soil conditions [1]. On the other hand, backscatter maps can also be exploited in the field of quantization. In the last decades, innovative spaceborne radar techniques have been proposed in order to brake the limitations imposed by "conventional" SAR systems and to acquire wider swaths with finer azimuth resolutions. Clearly, the consequent increase in the amount of information implies harder requirements in terms of on-board memory and downlink capacity. This has motivated the investigation of advanced quantization strategies in order to meet a trade-off between the quality of the resulting SAR products and the sensor acquisition capabilities. In this framework, a novel performance-optimized block-adaptive quantization (PO-BAQ) method [2], which exploits the availability of global backscatter maps, has been proposed in order to extend the concept of the state-of-the-art BAQ and to optimize the resource allocation together with the resulting interferometric performance. As a consequence, large-scale mosaics of backscatter images gain a central role in the generation of SAR backscatter maps and allow for the global monitoring of the Earth's environmental change as well as the generation of bitrate maps for advanced quantization strategies.

Radar backscattering is defined as the portion of a radar signal which is redirected back to the radar antenna after an interaction with a target on the ground. Its properties depend on several factors, which are related to the instrument itself, such as frequency, polarization, and acquisition geometry, as well as to the characteristics of the illuminated on-ground area, such as soil conditions, surface roughness, and scene topography. Different quantities are usually exploited to represent SAR backscatters, as described in [3] and [4]. However, the radar brightness β^0 is the only one that does not require a precise knowledge of the local incidence angle. In order to avoid mistakes due to limited knowledge of ground topography (which direct impacts on the estimation of the local incidence angle), β^0 will be used in this work as radar backscatter reference quantity.

Several models can be found in the literature to characterize the backscatter behaviour depending on sensor parameters and target properties. Well known and widely used in the scientific community are the ones provided by Ulaby and Dobson in 1989 [3]. Moreover, the availability of a large amount of high-quality SAR data provided by

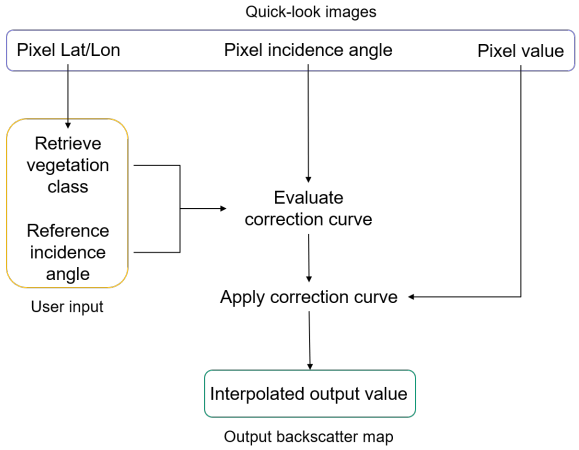

Figure 1 Algorithm flowchart. The output backscatter map is referred to a precise reference incidence angle.

the TerraSAR-X (TSM) and TanDEM-X (TDM) missions allows for a precise statistical analysis of X-band backscatters from space, depending on specific system parameters and on-ground target properties, such as polarization, vegetation class, local incidence angle, acquisition and seasonal time [1].

This paper is structured as follows. Section 2 shows the procedure for the generation of SAR backscatter maps, focusing on the interpolation algorithm to the output reference incidence angle and on the dedicated algorithm required for filling the missing values. Section 3 describes the application of the PO-BAQ as example of future quantization enhancement thanks to a priori knowledge of SAR backscatter statistics. Finally, the conclusions are drawn in Section 4.

2 Backscatter Map Generation Algorithm

The objective of this work is the generation of a global X-band backscatter map from TerraSAR-X (TSX) and TanDEM-X (TDX) quick-look images [5]. Quick-look products are generated as bypass data by the TanDEM-X operational processor (ITP). They provide less resolution compared to standard single-look slant-range complex products (SSC Level-1b)[6] and are radiometrically calibrated according to the specified absolute calibration factor. Also, they are geocoded into latitude/longitude coordinates and are provided together with the associated matrix of local incidence angles. The interpolation algorithm is applied depending on the acquisition incidence angle and vegetation class; the output backscatter map has thus to be referred to a precise reference incidence angle α_{ref}. The algorithm flowchart is shown in Figure 1. The input β^0 values, associated to different local incidence angles and vegetation classes, are interpolated to a specified output reference incidence angle by using the Ulaby backscatter models [3]. In particular, each input β^0 pixel is associated to a vegetation class. In this work, the *GLOBCOVER* classification map [7], provided by ESA in a resolution of 300 x 300 m^2, is used. In the final paper we will update the work with the newly released GLOBCOVER 2020 map at 10 m resolution [8]. Since the land cover classes provided by ESA differ from the Ulaby ones, an intermediate step is required in order to associate the *GLOBCOVER* classes with similar statistics to the same Ulaby model [1]. This land cover mapping is reported in Table 1. The interpolation is performed by evaluating the acquisition incidence angle of the β^0 pixel. A correction factor is thus derived depending on the output reference incidence angle α_{ref} and vegetation class and is then applied to the β_0 value. In particular, the correction of an input pixels β^0_{in}, associated to an acquisition incidence angle α_{in} and to a specific vegetation class, is performed as:

$$\beta^0_{\alpha_{ref}} = \beta^0_{\alpha_{in}} I(\Delta\alpha) \quad (1)$$

where $\beta^0_{\alpha_{ref}}$ is the pixel radar brightness of the output cell, *I* identifies the incidence-angle-dependent correction curve associated to a specif vegetation class, while $\Delta\alpha$ is defined as:

$$\Delta\alpha = \alpha_{in} - \alpha_{ref} \quad (2)$$

Table 1 Mapping between the *GLOBCOVER* classification map provided by ESA and the land cover classes of the Ulaby models.

GLOBCOVER classification map	**Ulaby model**
Closed to open (>15%) broadleaved evergreen or semi-deciduous	Trees
Closed (>40%) broadleaved deciduous forest (>5m)	
Open (15-40%) broadleaved deciduous forest/woodland	
Closed (>40%) needleleaved evergreen forest (>5m)	
Open (15-40%) needleleaved deciduous or evergreen forest (>5m)	
Closed to open (>15%) mixed broadleaved and needleleaved forest (>5m)	
Sparse (<15%) vegetation	
Closed to open (>15%) broadleaved forest regularly flooded	
Post-flooding or irrigated croplands (or acquatic)	Grasses
Rainfed croplands	
Mosaic grassland (50-70%) / forest or shrubland (20-50%)	
Closed to open (>15%) herbaceous vegetation (grassland, savannas or lichens/mosses)	
Closed to open (>15%) grassland or woody vegetation on regularly flooded or waterlogged soil	
Mosaic forest or schrubland (50-70%) / grassland (20-50%)	Shrubs
Closed to open (>15%) (broadleaved or needleleaved, evergreen or deciduous) shrubland	
Closed (>40%) broadleaved forest or shrubland permanently flooded - Saline or brackish water	
Artificial surfaces and associated areas (urban areas >50%)	Roads
Bare areas	Soil & Rocks
Permanent snow and ice	Dry Snow
Mosaic cropland (50-70%) / vegetation (grassland/shrubland/forest) (20-50%)	Short Vegetation
Mosaic vegetation (grassland/shrubland/forest) (50-70%) / cropland (20-50%)	
Water bodies	None

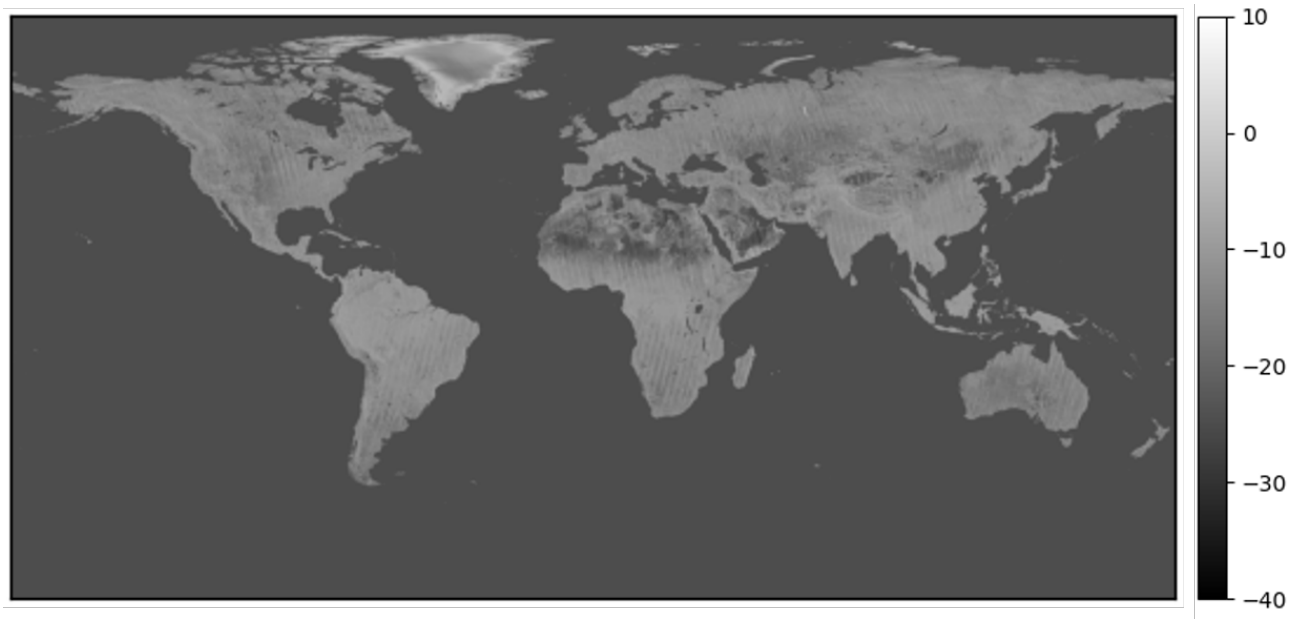

Figure 2 X-band global backscatter map without gaps, i.e., after missing values interpolation. Backscatter mean value in dB referred to HH polarization and to 40° output reference incidence angle.

Note that, doing so, backscatter maps can be generated for any output reference incidence angle, starting from the same input data. As described in the previous section, the availability of a large amount of SAR data, e.g., several acquisitions over the same ground area at different dates, allows for a statistical analysis of X-band backscatters. Several statistics can be thus derived from the *n* pixels contributing to the same output cell:

1. backscatter mean value, defined as the average of the *n* interpolated $\beta^0_{\alpha_{ref}}$ values;
2. backscatter standard deviation, defined as the sample standard deviation of the *n* $\beta^0_{\alpha_{ref}}$ values within the same output resolution cell;
3. backscatter maximum/minimum value, evaluated as the maximum/minimum value of the population of the *n* interpolated $\beta^0_{\alpha_{ref}}$ values;
4. backscatter population, defined as the number of input values contributing to the same output resolution cell, i.e., *n*;
5. backscatter 90^{th} percentile, evaluated as the upper/lower bound of the 90% distribution of the *n* interpolated $\beta^0_{\alpha_{ref}}$ values.

The above mentioned statistics can be exploited for different purposes. For instance, the mean value can be used for performance estimation, while the standard deviation map can be seen as a measure of the backscatter dynamic and can be therefore used for quantization tasks [9]. Also, the maximum/minimum value can be useful for the evaluation of saturation levels in order to avoid clipping, while the evaluation of the 90^{th} percentile aims to ignore infrequent peaks and thus to give a more reliable estimation of the backscatter distribution.

In order to face to the lack of data in several regions, a dedicated algorithm has been also integrated for filling the empty output cells. As first step, SAR data acquired with different polarizations, i.e., VV and HV, can be exploited and interpolated to HH polarization and to the required reference incidence angle, according to Ulaby models. Otherwise, the *GLOBCOVER* classification map, together with the Ulaby models, can be used to directly fill the missing gaps. Anyway, given at least the two available global coverages of TanDEM-X, remaining voids represent a very small percentage (less than 0.1%) of all landmasses.

Figure 2 shows the X-band global backscatter map referred to HH polarization and to 40° output reference incidence angle. Note that the map refers to backscatter mean values and has a final posting of 5 x 5 km^2 at the equator, corresponding to an angular spacing of 0.05° in latitude/longitude coordinates. The gaps have been already filled according to the dedicated algorithm described above.

3 Performance-Optimized Block-Adaptive Quantization (PO-BAQ)

Performance-optimized block-adaptive quantization (PO-BAQ) [2] is a novel quantization technique aiming at the optimization of the resource allocation of the state-of-the-art quantization algorithm, i.e., BAQ. It was born from the need of handling a large amount of data, in terms of on-board memory and downlink capability, for future SAR systems which will brake the "conventional" limitations of acquiring larger swaths with finer azimuth resolutions. According to this quantization strategy, the bitrate $N_{b,req}$ required for SAR raw data compression can by estimate as:

$$N_{b,req} = f(\zeta_{req}, \sigma_{\beta_0}, N_l, N_{acq}). \quad (3)$$

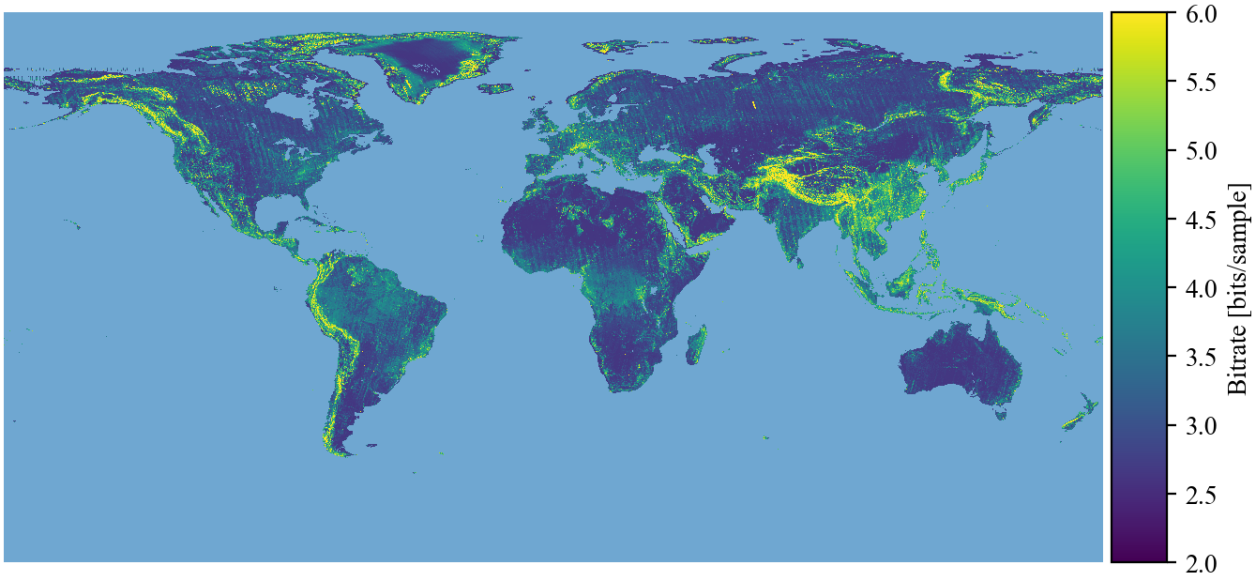

Figure 3 Global bitrate map resulting from a requirement on the interferometric phase error of $\sigma_{\Delta\varphi_q} = 5°$.

In the equation above, ζ_{req} identifies the requirement imposed on the quantization performance, which can be defined in terms of signal-to-quantization-noise ratio (SQNR), coherence loss or interferometric phase error; N_l is the number of looks, given by the system resolution and the target posting, and N_{acq} is the number of available acquisitions, which is usually defined at mission planning and can be interpreted as a sort of "temporal" looks. Finally, σ_{β_0} represents the local backscatter standard deviation computed over the theoretical integration area of

$$A_{SAR} = L_{chirp} \times L_s; \tag{4}$$

L_{chirp} is the chirp length and L_s is the synthetic aperture of the radar which, in turn, are defined as

$$L_{chirp} = \frac{c\tau_p}{2}, L_s = \lambda \frac{R_0}{L_a}, \tag{5}$$

where c is the speed of light, τ_p stays for the chirp pulse duration, R_0 is the slant range and L_a is the physical antenna dimension along azimuth. The local backscatter standard deviation can be derived from the generated backscatter maps, and in general has to be available a priori before a data take. Moreover, the function *f(.)* in (3) has to be precisely described from a statistical characterization of the performance degradation using real data, as described in [2]. In particular, it describes the quantization performance degradation as a function of the bitrate N_b and of the backscatter statistics σ_{β_0}. Once all the input parameters and the function *f(.)* in (3) are known, a bitrate map can be derived as

$$N_{b,req} = \underset{N_b \in [N_{b,min}, N_{b,max}]}{\operatorname{argmax}} \{\zeta(N_b, N_l, N_{acq}, \sigma_{\beta_0}) \leq \zeta_{req}\} \tag{6}$$

where $N_{b,min}$ and $N_{b,max}$ are the minimum and maximum allowed bitrates, respectively, which are usually set at system/instrument design level.

As presented in [2], variable bitrate maps can be derived depending on target performance parameters, such as the interferometric phase error or the SQNR. An example of global bitrate map, resulting from a requirement on the interferometric phase error of $\sigma_{\Delta\varphi_q} = 5°$ is shown in Figure 3. The input X-band standard deviation map has been generated as described in Section 2 with a final resolution of 5 x 5 km^2 at the equator, i.e., corresponding to an angular spacing of 0.05° along both latitude and longitude. Note that a large dispersion in terms of required bitrate is present, ranging from about 2.5 bits/sample to 6 bits/sample.

4 Conclusions

In this paper, the generation of a global X-band backscatter map from TSX and TDX quick-look images has been discussed. The interpolation approach using the Ulaby models has been also presented, together with a dedicated algorithm for filling the missing values. Moreover, the benefits of a statistical analysis of X-band SAR backscatters for future SAR systems has been discussed, especially in the field of quantization. A novel PO-BAQ method has been applied as example of novel quantization strategy, in order to point out the importance of a priori knowledge of global backscatter maps for the optimization of future SAR systems. Some preliminary results have been shown in a final output resolution of 5 x 5 km^2 at the equator. In the final paper, global X-band backscatter maps will be generated with a final posting of 50 m in both azimuth and ground range, and corresponding bitrate maps will be provided at the same output cell resolution. Moreover, the new *WORLDCOVER* classification map released by ESA in a resolution of 10 m [8] will be investigated and hopefully used as input for the retrieval of vegetation classes in the backscatter map algorithm.

5 Literature

[1] P. Rizzoli, B. Brautigam, S. Wollstadt, and J. Mittermayer, “Radar backscatter mapping using TerraSAR-X,” *IEEE Trans. Geosci. Remote Sens.*, vol. 49, no. 10, pp. 3538–3547, 2011.

[2] M. Martone, N. Gollin, P. Rizzoli, and G. Krieger, "Performance-Optimized Quantization for InSAR Applications." *EUSAR 2021; 13th European Conference on Synthetic Aperture Radar*. VDE, 2021.

[3] F. T. Ulaby and M. C. Dobson, *Handbook of Radar Scattering Statistics for Terrain*. Norwood, MA: Artech House, 1989.

[4] D. Small, N. Miranda, and E. Meier, “A revised radiometric normalization standard for SAR,” in *Proc. IGARSS*, Cape Town, South Africa, 2009, pp. IV-566–IV-569.

[5] T. Fritz, M. Eineder, H. Breit, B. Schättler, E. Boerner, and M. Huber, “The TerraSAR-X basic products—Format and expected performance,” presented at the *Eur. Conf. Synthetic Aperture Radar*, Dresden, Germany, 2006.

[6] T. Fritz and M. Eineder, TerraSAR-X Ground Segment Basic Product Specification Document, no. 1.6, Mar. 18, 2009.

[7] GLOBCOVER Products Description Manual. [Online]. Available: http://due.esrin.esa.int/files/GLOBCOVER2009_Validation_Report_2.2.pdf

[8] WORLDCOVER 2020 land cover product. [Online]. Available: https://esa-worldcover.org/en

[9] J. Mittermayer, M. Younis, R. Metzig, S. Wollstadt, J. Márquez, and A. Meta, “TerraSAR-X system performance characterization and verification,” *IEEE Trans. Geosci. Remote Sens.*, vol. 48, no. 2, pp. 660–676, Feb. 2010.